ORIGINAL PAPER

Overexpression of Hsp27 ameliorates symptoms of Alzheimer's disease in APP/PS1 mice

Melinda Erzsébet Tóth · Viktor Szegedi · Edina Varga · Gábor Juhász ·
János Horváth · Emőke Borbély · Balázs Csibrány · Róbert Alföldi ·
Nikolett Lénárt · Botond Penke · Miklós Sántha

Abstract Hsp27 belongs to the small heat shock protein family, which are ATP-independent chaperones. The most important function of Hsp27 is based on its ability to bind non-native proteins and inhibit the aggregation of incorrectly folded proteins maintaining them in a refolding-competent state. Additionally, it has anti-apoptotic and antioxidant activities. To study the effect of Hsp27 on memory and synaptic functions, amyloid-β (Aβ) accumulation, and neurodegeneration, we generated transgenic mice overexpressing human Hsp27 protein and crossed with APPswe/PS1dE9 mouse strain, a mouse model of Alzheimer's disease (AD). Using different behavioral tests, we found that spatial learning was impaired in AD model mice and was rescued by Hsp27 overexpression. Electrophysiological recordings have revealed that excitability of neurons was significantly increased, and long-term potentiation (LTP) was impaired in AD model mice, whereas they were normalized in Hsp27 overexpressing AD model mice. Using anti-amyloid antibody, we counted significantly less amyloid plaques in the brain of APPswe/PS1dE9/Hsp27 animals compared to AD model mice. These results suggest that overexpression of Hsp27 protein might ameliorate certain symptoms of AD.

M. E. Tóth (✉) · V. Szegedi · B. Csibrány · R. Alföldi ·
N. Lénárt · M. Sántha
Institute of Biochemistry, Biological Research Centre of the
Hungarian Academy of Sciences, Temesvari Ave. 62,
6726 Szeged, Hungary
e-mail: toth.e.melinda@gmail.com

E. Varga · G. Juhász · J. Horváth · E. Borbély · B. Penke
Deparment of Medical Chemistry, Faculty of Medicine, University
of Szeged, Dóm Square 11,
Szeged, Hungary

Introduction

AD is one of the most common neurodegenerative diseases, and its prevalence is strongly correlated with aging (Evans et al. 1989). AD is characterized by progressive loss of memory and cognitive functions (McKhann et al. 1984). The pathological hallmarks of AD are extracellular amyloid plaque deposition, formation of intracellular neurofibrillary tangles, and other alterations in the brain such as activation of microglial cells, oxidation of lipids, induction of reactive oxygen species, disruption of neuronal metabolic homeostasis, and neuronal cell death (Serrano-Pozo et al. 2011; Monji et al. 2001). Amyloid plaques and neurofibrillary tangles are present mainly in brain regions involved in learning, memory, and emotional behaviors, primarily in the hippocampus (Mattson 2004).

Heat shock proteins (Hsps) are ubiquitously expressed evolutionary conserved proteins which are upregulated by different stressors and also in various pathological conditions. Most of the stress-induced proteins are molecular chaperons, and they have an essential role in biosynthesis, transport, translocation, folding, and assembly of other proteins (Morimoto et al. 1992). Under stress, Hsps prevent protein misfolding and oligomerization, and they transfer misfolded proteins to the proteasome for degradation (Becker and Craig 1994). They also assist in the maintenance of normal cellular homeostasis and metabolism.

Hsp27 belongs to the small heat shock protein (sHsp) family, which are ATP-independent chaperones (Jakob et al. 1993). The most important function of sHsps is that they can

Springer

inhibit the aggregation of incorrectly folded proteins by binding to non-native proteins, and maintain them in a refolding-competent state (Haslbeck and Buchner 2002). Moreover, they also have anti-apoptotic and antioxidant activities and can bind to the actin cytoskeleton and stabilize it (Arrigo et al. 2002, Preville et al. 1999, Wang and Spector 1996).

Hsps are upregulated in several neurodegenerative diseases and can protect brain cells against free radical injury, oxidative stress, and misfolded proteins (Kalmar and Greensmith 2009). Several studies indicate that chaperones are potent suppressors of neurodegeneration and are, therefore, promising therapeutic targets for protein conformational disorders (reviewed in Muchowski and Wacker 2005). For example, treating a polyglutamine disease model with an antiulcer drug, geranylgeranylacetone (GGA), which can induce the expression of different Hsps, could suppress the accumulation of pathogenic proteins and ameliorate the related phenotype (Katsuno et al. 2005). In a rat model of Parkinson's disease, Hsp104 was found to be similarly efficient (Lo Bianco et al. 2008). An increased level of expression of small Hsps and Hsp70 in the brain of AD patients has been reported in a number of studies (Perez et al. 1991; Muchowski and Wacker 2005). Several studies suggest that expression of Hsps could suppress the progression of AD (Magrané et al. 2004; Muchowski and Wacker 2005; Evans et al. 2006). Hoshino et al. (2011) investigated the effect of overexpression of Hsp70 on AD-related phenotypes, using double transgenic mice overexpressing Hsp70 and a mutant (Swedish) type of APP (APPswe). They demonstrated that overexpression of Hsp70 inhibited the development of the pathological phenotype of AD and the resultant cognitive deficit, possibly through its effects on antiaggregation, neuroprotection, and stimulation of Aβ clearance.

To study the effect of a small heat shock protein, Hsp27, on memory and synaptic functions, Aβ accumulation, and neurodegeneration, we generated transgenic mice overexpressing the human Hsp27 protein and crossed them with the APPswe/PS1dE9 mouse strain, a widely used mouse model of AD.

Materials and methods

Animals

The study conformed to EU Directive 2010/63/EU and was approved by the regional Station for Animal Health and Food Control (Csongrád, Hungary) under project license XVI/02752/2009. Mice were housed in groups of two to three under standard conditions (24 °C, 12 h light–dark cycle) with food and water available ad libitum.

Generation of APPswe/PS1dE9/Hsp27 transgenic mice

We have previously generated transgenic mice overexpressing the human Hsp27 protein on FVB genetic background (Tóth et al. 2010). Transgenic DNA construct contained the human Hsp27 cDNA driven from a cytomegalovirus (CMV) promoter. This transgenic line was crossed with C57BL/6 mice four times in order to establish a Hsp27 transgenic line on a homogenous C57BL/6 genetic background. B6C3-Tg(APPswe/PS1dE9)85Dbo/Mmjax mice were purchased from The Jackson Laboratory (Bar Harbor, ME, USA) and maintained on C57BL/6 genetic background. Hsp27 transgenic mice then were crossed with APPswe/PS1dE9 mice to generate APPswe/PS1dE9/Hsp27 multiple transgenic strain. To identify the genotype of the offsprings, polymerase chain reaction (PCR) was performed from tail biopsies using the following primers: 5′-GTC CCT GGA TGT CAA CCA CT-3′ and 5′-GAC TGG GAT GGT GAT CTC GT-3′ for Hsp27; 5′-GAC TGA CCA CTC GAC CAG GTT CTG-3′ and 5′-CTT GTA AGT TGG ATT CTC ATA TCC G-3′ for APP(Swe); and 5′-AAT AGA GAA CGG CAG GAG CA-3′ and 5′-GCC ATG AGG GCA CTA ATC AT-3′ for PS1dE9. The PCR amplification was done in a MJ Research PTC-200 Thermal Cycler using the following parameters: denaturation at 95 °C for 4 min followed by 29 cycles of denaturation at 95 °C for 1 min, annealing at 56 °C for 1 min and elongation at 72 °C 1 min, and a final extension at 72 °C for 4 min.

Western blot analysis

Expression of Hsp27 was determined from cortical and hippocampal tissues of 7 months old transgenic mice and wild type littermates. For ApoA1 protein level estimation, whole brain tissue was used. Total protein was isolated from frozen tissues homogenized in lysis buffer (containing 50 mM Tris–HCl, 150 mM NaCl, 1 % Triton X-100, 0.5 % Na deoxycholate, 0.1 % SDS, and protease inhibitor), centrifuged at 10,000 rpm for 10 min at 4 °C, and the supernatant was used for western blot analysis. Protein concentration was measured at 280 nm using a NanoDrop spectrophotometer (NanoDrop Technologies). Protein samples (50 μg) were separated by 10 % SDS-PAGE (Cambrex) and transferred electrophoretically onto Hybond-P PVDF membrane (Amersham). Membrane was blocked for 1 h in 5 % milk powder. After a short wash in PBS-Tween buffer, membrane was incubated with anti-Hsp27 (1:500, Stressgen, Cat No: SPA-803), anti-ApoA1 (1:250, Rockland, Cat. No: 600-101-196), and anti-β-actin (1:1,400, Sigma, Cat. No: A2103) antibodies overnight at 4 °C. After a brief wash, membranes were incubated with anti-goat (1:10,000, Jackson ImmunoResearch, Cat. No: 305-035-003) or anti-rabbit (1:35,000, Jackson ImmunoResearch, Cat. No: 111-035-003) secondary antibodies for 45 min at

room temperature. Signals were developed using Luminata Forte Western HRP Substrate (Millipore) according to the manufacturer's instructions. Signal intensities were quantified using ImageJ 1.45 software.

Behavioral tests

For behavioral testing, 7-month-old male mice were used. Before starting the tests, mice were handled daily for 2 weeks. Behavioral tests were performed between 9:00 a.m. and 4:00 p.m. Tests were recorded by video camera, and data were analyzed by EthoVision 2002 computer-controlled video tracking system (The Noldus Information Technology, The Netherlands).

Open field

Locomotor activity and anxiety-like behavior were studied using open field test. Each mouse was placed in the center of a plastic oval arena ($50 \times 70 \times 30$ cm) virtually divided into central and peripheral areas by the software. Total distance travelled (in centimeters), number of rearings, time spent with grooming, and time spent in the peripheral areas were measured. Data were collected for 5 min. All animals were tested once.

Barnes maze test

In the Barnes maze test, using a bright light, animals were reinforced to escape from the open platform surface to a small dark chamber located under the platform called "target box." The experiment was performed according to a technique published on the internet (Sunyer et al. 2007). The maze consisted of a circular platform (100 cm in diameter) with 20 holes (hole diameter, 5 cm) along the perimeter. The circular open field was elevated 90 cm from the floor. A black escape (target) box ($19 \times 6 \times 7$ cm) was located under one of the holes. The location of the target box was consistent for any given mouse, but was randomized across mice. The platform was surrounded by curtains and visual cues on it to help the mice with orientation. Mice were placed in the middle of the maze and were free to explore it. The trial ended after 3 min or when the mouse entered the escape box. When a mouse entered the escape box, it was allowed to stay in it for 1 min. If the mouse did not find the escape box, it was guided to it and left inside for 1 min. One trial per day was performed for five consecutive days. Time of latency to enter the target box was measured. On day 8, the probe trial was performed without the escape box to confirm that this spatial task was acquired based on navigation using distal-environment room cues. The trial ended after 2 min. Time of latency to reach the target hole was measured.

Morris water maze test

For the Morris water maze test, a circular pool (130 cm in diameter and 60 cm in height) was filled to a height of 45 cm with water. Water temperature was maintained between 22 °C and 23 °C, and it was made opaque by mixing milk in it. For the invisible platform test, a white colored platform (5 cm in diameter) was placed at the center in one of four quadrants of the pool (training quadrant) and submerged 1 cm below the water surface so that it was invisible at water level. The pool was surrounded by curtains, and different spatial cues were attached to the curtains to help the mice with orientation. The location of the platform was fixed at the same quadrant while the start position of swimming was varied. Mice were given two trials per day for five consecutive days, during which they were allowed to find the platform within 90 s. Once the mouse located the platform, it was permitted to stay on it for 10 s. If the mouse did not find the platform within 90 s, it was guided to the platform and placed on it for 10 s. The escape latency, the time required for the mouse to find and climb onto the platform, was recorded. The means of the data from each day were used for statistics. Some of the mice have shown floating behavior in the Morris water maze test. This means that mice remained motionless most of the time during the trial period. These mice were also very passive in the Barnes maze test. We counted the trials when mice showed floating/passive behavior and found that three mice were motionless almost in the 70 % of trials; therefore, these mice were excluded from the behavioral tests.

Immunohistochemistry

Subsequent to the behavioral tests, mice were sacrificed by cervical dislocation, and the brains were removed for further studies. Frozen sections (10 μm) of the brains were processed for immunohistochemistry. Sections were fixed in acetone for 3 min. After a brief wash with PBS, sections were incubated with 1.5 % H_2O_2 in methanol for 20 min then with 3 % H_2O_2 for 20 min to block endogenous peroxidases. PBS wash was followed by collagenase treatment using 0.1 mg/ml collagenase type II (Sigma) in a buffer containing 0.25 M NaCl, 50 mM Tris–HCl, pH 7.4, and 1 mM EDTA at 37 °C for 5 min. After a brief wash in PBS, sections were incubated in 5 % goat serum for 1 h at room temperature to prevent nonspecific binding of the antibody. Sections were then covered with anti-Aβ [1–42]

(1:60, Invitrogen, Cat No. 700254), anti-cleaved caspase-3 (1:50, Cell Signalling, Cat. No. Asp-175), or with anti-Hsp27 (1:50, Stressgen, Cat No: SPA-803) primary antibodies overnight at 4 °C. Slides were washed with PBS, then goat anti-rabbit secondary antibody (1:150, Jackson ImmunoResearch, Cat. No.111-035-003) was applied for 45 min. After washing, slides were incubated with developing reagent (10 % dimethyl formamide, 10 % imidazole, 0.02 % aminoethyl carbazole, 0.04 % H_2O_2) at room temperature until the brown color appeared (approximately 10 min). Sections were then counterstained with hematoxylin solution for 2 min at room temperature followed by washing with PBS, and they were covered with glycerol gelatin.

For Aβ [1–42] and cleaved capase-3 antibody stainings, 7-month-old transgenic ($n=6$) and wild type ($n=6$) animals were used. Stained sections were photographed using a light microscope equipped with CCD camera, and amyloid plaques or apoptotic cells were counted in 15 microscopic fields by two independent individuals.

Fluoro-Jade C staining

Brains were removed, and 10-μm acetone-fixed frozen sections were prepared. Slides were immersed into absolute ethanol for 5 min, then rinsed in 70 % ethanol for 2 min, in 30 % ethanol for an additional 2 min, and finally in distilled water for 2 min. Sections then were incubated in 0.06 % potassium permanganate solution for 30 min. Following a 2-min water rinse, sections were transferred into a 0.0004 % solution of Fluoro-Jade C (Chemicon) fluorescent dye dissolved in 0.1 % acetic acid. Slides were washed three times in distilled water for 1 min. After drying, sections were cleared in xylene for 2 min and coverslipped with DPX nonfluorescent mounting media. Degenerating neurons emitting green fluorescence were visualized under Nikon Eclipse E600 fluorescent microscope using a 520-nm fluorescein filter set. Six 7-month-old animals from each group were selected, and two slides of each animal's brain were stained using Fluoro-Jade C dye. On each slide, 15 digital photographs were taken, and degenerating neurons were counted by two independent individuals.

Hippocampal slice electrophysiology

Following standard procedures, 400-μm-thick transverse hippocampal slices were prepared from the brain of 7-month-old mice using a McIlwain tissue chopper (Campden Instruments, Loughborough, UK). Slices were incubated in standard artificial cerebrospinal fluid (ACSF) at ambient temperature for 60 min, which was constantly gassed with 95 % O_2–5 % CO_2. ACSF contained (millimolar) NaCl, 130; KCl, 3.5; $CaCl_2$, 2; $MgCl_2$, 2; NaH_2PO_4, 0.96; $NaHCO_3$, 24; D-glucose, 10 (pH 7.4). Individual slices were transferred to a 3D-MEA chip with 60 tip-shaped and 60-μm-high electrodes spaced by 200 μm (Ayanda Biosystems, S.A., Lausanne, Switzerland). The slice was continuously perfused with oxygenated ACSF (1.5 ml/min at 36 °C) during the whole recording session. Data were recorded by a standard, commercially available MEA setup (Multi-Channel Systems MCS GmbH, Reutlingen, Germany). The Schaffer collateral was stimulated by injecting a biphasic voltage waveform (−100/+100 μs) through one selected electrode at 0.033 Hz. Care was taken to choose the stimulating electrode in the same region from one slice to the other. The peak-to-peak amplitudes of fEPSPs at the stratum pyramidale and stratum radiatum of CA1 were analyzed. After a 30-min incubation period, the threshold and the maximum of stimulation intensity for evoked responses was determined. For evoking responses, 30 % of the maximal stimulation intensity was used.

Following a stable 10-min control sequence, the stimulus intensity was continuously increased from 400 to 3,200 mV with 400 mV steps (input/output curve). Paired-pulse protocol consisted of two stimulation pulses injected with interstimulus intervals of 20, 50, 200, and 500 ms with 0.033 Hz. Three data points were obtained at every stimulation intensity/interstimulus intervals at the input/output curve and paired-pulse protocol. LTP was induced using a theta-burst stimulation (TBS) pattern applied at the maximum stimulation intensity. TBS comprised a train with ten bursts given at 5 Hz per train and four pulses given at 100 Hz per burst.

RNA extraction and quantitative real-time PCR

For quantitative real-time PCR (Q-PCR), 6-month-old Hsp27 transgenic ($n=3$) and wild type mice ($n=3$) were used. Total RNA was extracted from whole brain using Trizol reagent (Invitrogen), according to the manufacturer's protocol. RNA samples then were cleaned using NucleoSpin RNA Clean-up columns (Macherey-Nagel) and treated with DNaseI (Macherey-Nagel) for 30 min. First-strand cDNA was synthesized by reverse transcription (5 μg RNA/30 μl reaction volume) using High-Capacity cDNA Archive kit (Applied Biosystems). The temperature profile of the reaction was as follows: 10 min at room temperature, 2 h at 37 °C, 5 min on ice, and finally, 10 min at 75 °C.

Q-PCR was performed on a RotorGene 3000 instrument (Corbett Research, Sydney, Australia) using gene-specific primers listed in Table 1. The cDNA was diluted 1:20, and 9 μl of this mix was used as a template in the reaction.

Table 1 List of Q-PCR primers used in this study

Gene	Forward primer	Reverse primer
Amyloid precursor protein (APP)	TACTGCATGGCGGTGTGT	CGTGGGAAGTTTATCAGGATCT
Apolipoprotein-AI (ApoAI)	TATGTGGATGCGGTCAAAGA	TGAACCCAGAGTGTCCCAGT
Apolipoprotein-D (ApoD)	GAAGGCTTTTACAGGCTCCA	GGCCAGGAACATCAGCAT
Apolipoprotein-E (ApoE)	CAATTGCGAAGATGAAGGCTC	TAATCCCAGAAGCGGTTCAG
Nitric oxide synthase-1 (Nos1)	CATCAGGCACCCCAAGTT	CAGCAGCATGTTGGACACA
Nitric oxide synthase-3 (Nos3)	CCAGTGCCCTGCTTCATC	GCAGGGCAAGTTAGGATCAG
LDL receptor-related protein-1 (Lrp1)	ACCACCATCGTGGAAAATG	GTCCCAGCCACGGTGATA
LDL receptor-related protein-2 (Lrp2)	GATGGATTAGCCGTGGACTG	TCCGTTGACTCTTAGCATCTGA
Low-density lipoprotein receptor (LDLr)	CAAGAGGCAGGGTCCAGA	CCAATCTGTCCAGTACATGAAGC
Heat shock protein 90 (Hsp90)	GTCTCGTGCGTGTTCATTCA	CATTAACTGGGCAATTTCTGC

Reactions were performed in a total volume of 20 µl containing 10 µl of FastStart SYBR Green Master mix (Roche) and 5 mM of each primer. The amplification was carried out with the following cycling parameters: 15 min heat activation at 95 °C, followed by 45 cycles denaturation at 95 °C for 25 s, annealing at 60 °C for 25 s, and extension at 72 °C for 20 s. Fluorescent signals were collected after each extension step at 72 °C. Relative expression ratios were normalized to β-actin.

Statistical analysis

All data obtained in this experiment were expressed as mean ± SEM. Statistical analysis was performed by one-way analysis of variance (ANOVA) followed by Fisher's post hoc test using OriginPro8 software. Electrophysiological data were analyzed by two-way ANOVA followed by Tukey's post hoc test. The level of statistical confidence was set at $p<0.05$.

Results

Generation of transgenic mice

Transgenic mice overexpressing the human Hsp27 protein were generated in our laboratory as described earlier (Tóth et al. 2010). By crossing the human Hsp27 overexpressing mice with the APPswe/PS1dE9 mouse strain, we generated a triple transgenic mouse strain. The APPswe/PS1dE9 strain (The Jackson Laboratory, Bar Harbor, ME, USA) is a widely used mouse model of AD (Jankowsky et al. 2004, Reiserer et al. 2007, Hamilton and Holscher 2012), and it shows several symptoms of the disease including impaired spatial learning, reduced long-term potentiation, widespread amyloid deposition, and mild neurodegeneration (The Jackson Laboratory (2013)) (http://jaxmice.jax.org/strain/004462.html). First, cerebral expression of the Hsp27 transgene was

investigated. Using western blot analysis, robust expression of human Hsp27 was detected in the cortical and hippocampal tissues of Hsp27 and triple transgenic (AD/Hsp) brains, while no expression was found in wild type and APPswe/PS1dE9 (AD) littermates (Fig. 1a). Hsp27 expression was also confirmed in the brain of Hsp27 and APPswe/PS1dE9/Hsp27 animals using immunohistochemical staining (Fig. 1b). While Hsp27 antibody stained hippocampal tissues of Hsp27 transgenics homogeneously, it showed a spotted, plaque-like staining pattern in the hippocampal region of APPswe/PS1dE9/Hsp27 brains (Fig. 1c).

Behavioral tests

Seven-month-old male mice were divided into three experimental groups: an AD mouse model group (APPswe/PS1dE9, $n=11$), an APPswe/PS1dE9/Hsp27 triple transgenic group ($n=12$), and a wild type group ($n=9$).

Locomotor activity

First, locomotor activity (total distance travelled), exploratory behavior (number of rearings), and anxiety (time spent on the periphery, time spent with grooming) were recorded using open field test. There was no significant difference between groups in these behavioral features (total distance travelled, $p=0.25$; rearings, $p=0.34$; time spent on periphery, $p=0.33$; grooming, $p=0.64$).

Barnes maze test

Spatial learning and memory were tested using Barnes maze and Morris water maze tests. Both tests are based on spatial navigation, and the performance of the animals depends on hippocampal function (Kennard and Woodruff-Pak 2011). In Barnes maze test, APPswe/PS1dE9 mice spent more than 130 s with searching the escape box on

Fig. 1 a Detection of human Hsp27 expression in the hippocampus and cortex of wild type (Wt), APPswe/PS1dE9 (AD), APPswe/PS1dE9/Hsp27 (ADHsp), and Hsp27 transgenic mice (Hsp27) using western blot analysis. b Hsp27 immunostaining of brain sections of 7 months old wild type (Wt), Hsp27 transgenic (Hsp27), APPswe/PS1dE9, and APPswe/PS1dE9/Hsp27 mice. Brown staining indicates human Hsp27 immunoreactivity (black arrows). Nuclei were counterstained with hematoxylin. Scale bar indicates 100 μm. c Higher magnification of the hippocampal region of Hsp27 transgenic and APPswe/PS1dE9/Hsp27 mice stained by anti-Hsp27 antibody. Black arrows indicate a plaque-like staining of Hsp27. Scale bar represents 100 μm
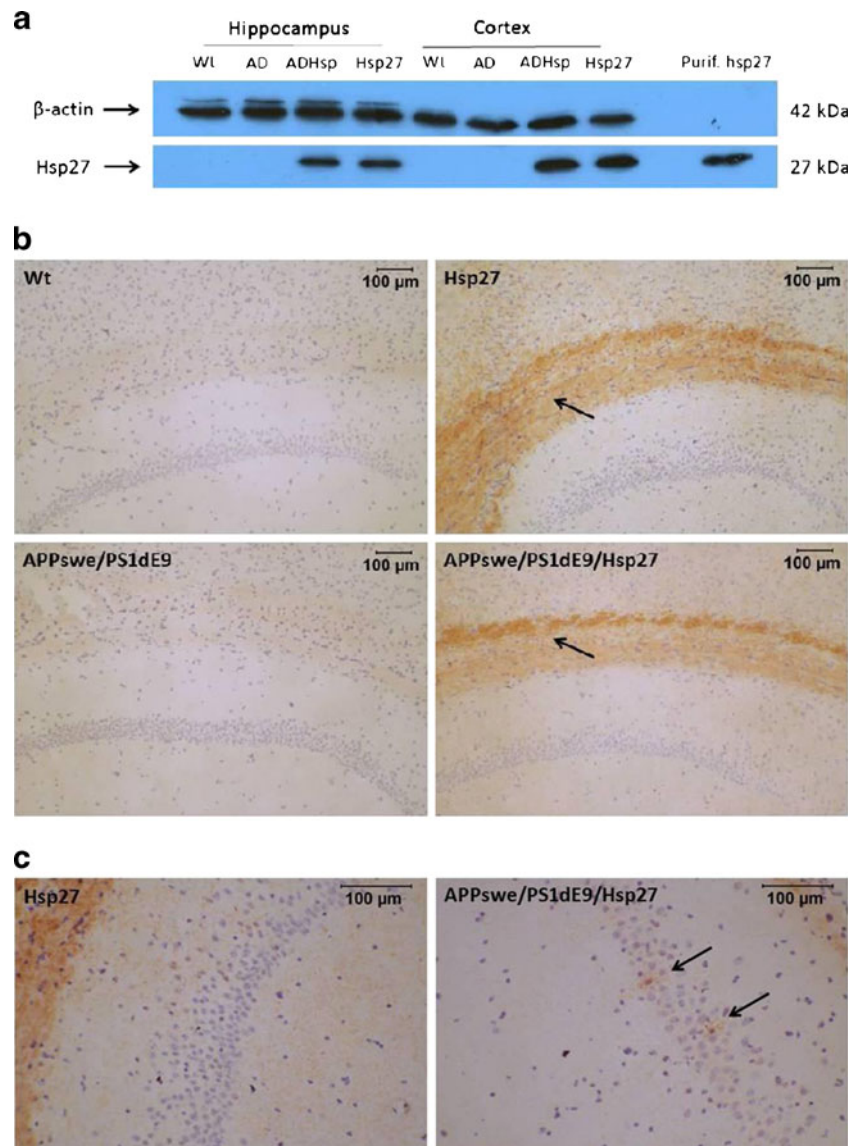

each day of the training period. In contrast, wild type and APPswe/PS1dE9/Hsp27 mice learned soon to find the escape hole as indicated by the reduction of escape latency. On the fourth day, mice from the wild type group spent 76 s with searching and performed significantly better than APPswe/PS1dE9 mice (140 s; $p<0.05$; Fig. 2a). However, there was no significant difference between the performance of wild type and APPswe/PS1dE9/Hsp27 mice. On the fifth day, the escape latency of the wild type and APPswe/PS1dE9/Hsp27 groups were 92 and 72 s, respectively, performing significantly better then APPswe/PS1dE9 mice (169 s; $p<0.01$ and $p<0.001$), and again, there was no significant difference between APPswe/PS1dE9/Hsp27 and wild type groups (Fig. 2a). The probe trial was performed 3 days after the last training session. The result of the probe trial was similar to the previous trial; wild type and APPswe/PS1dE9/Hsp27 mice found the correct target

hole within 50 and 41 s, respectively, and these were significantly shorter compared to APPswe/PS1dE9 mice (93 s; $p<0.05$ and $p<0.01$). No statistical difference was observed between wild type and APPswe/PS1dE9/Hsp27 groups (Fig. 2b).

Morris water maze test

Spatial learning was also tested using Morris water maze to confirm the result of Barnes maze test. On the third day, wild type mice find the escape platform in 41 s on average, and this was significantly shorter compared to APPswe/PS1dE9 group (76 s, $p<0.01$; Fig. 2c). On the fourth day, the escape latency of the wild type and APPswe/PS1dE9/Hsp27 groups was 52 and 50 s, respectively, performing significantly better than APPswe/PS1dE9 mice (74 s; $p<0.05$). There was no difference

Fig. 2 Assessment of learning and memory using behavioral assays. Cognitive behavior of 7 months old wild type (WT, n=9), APPswe/PS1dE9 (n=11), and APPswe/PS1dE9/Hsp27 (n=12) transgenic mice were compared. Escape latency in seconds during training session (a) and probe test of the Barnes maze test (b). Escape latency in seconds in Morris water maze test (c). Mean ± SEM is shown; *p<0.05; **p<0.01; ***p<0.001
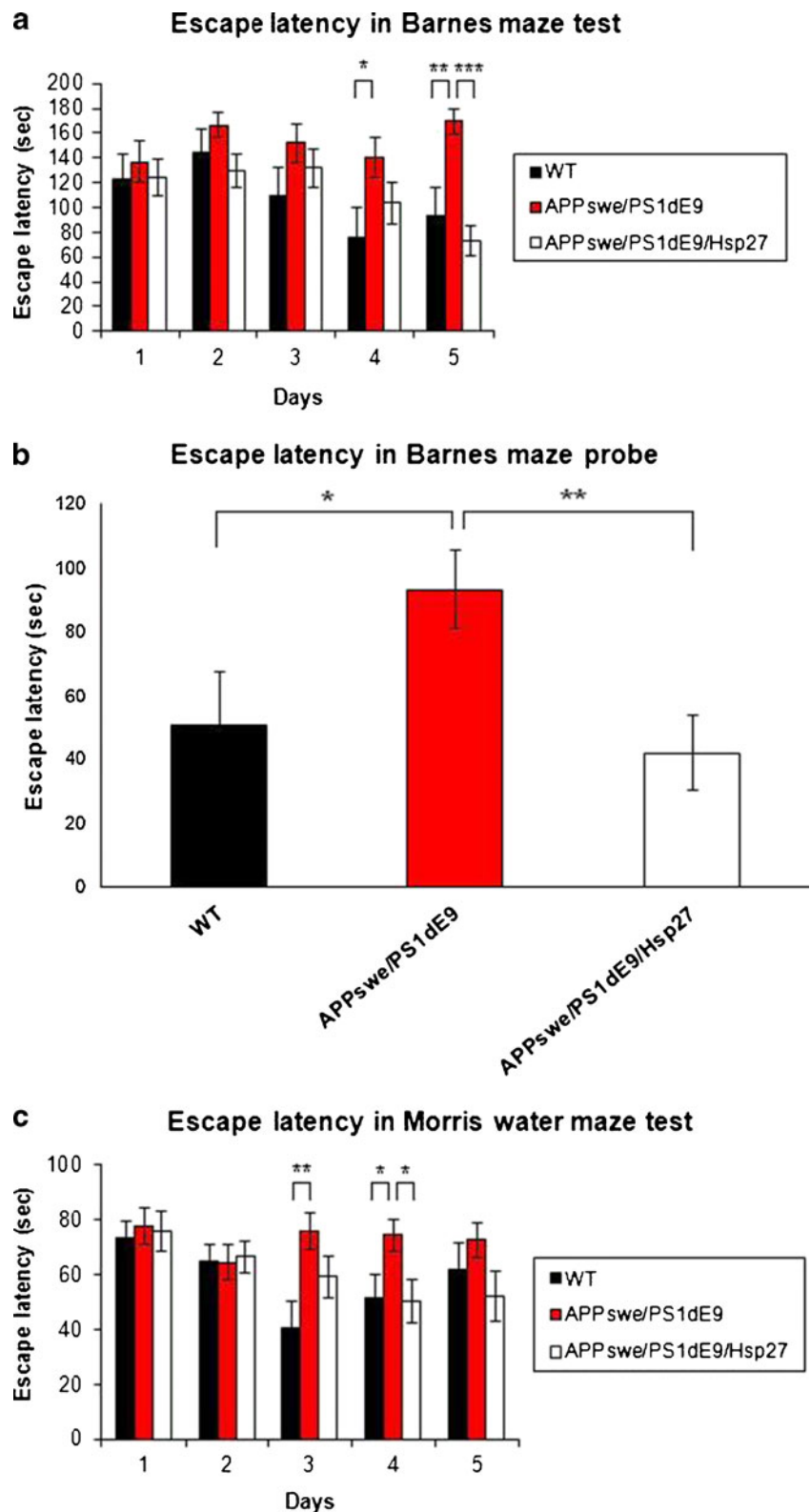
between the performance of APPswe/PS1dE9/Hsp27 and wild type groups (Fig. 2c). Interestingly, on the last day of training sessions, there was no statistical difference between groups, and the performance of most animals has declined.

Hippocampal slice electrophysiology

Hippocampal function was studied using paired-pulse facilitation (PPF) and long-term potentiation (LTP). Excitability
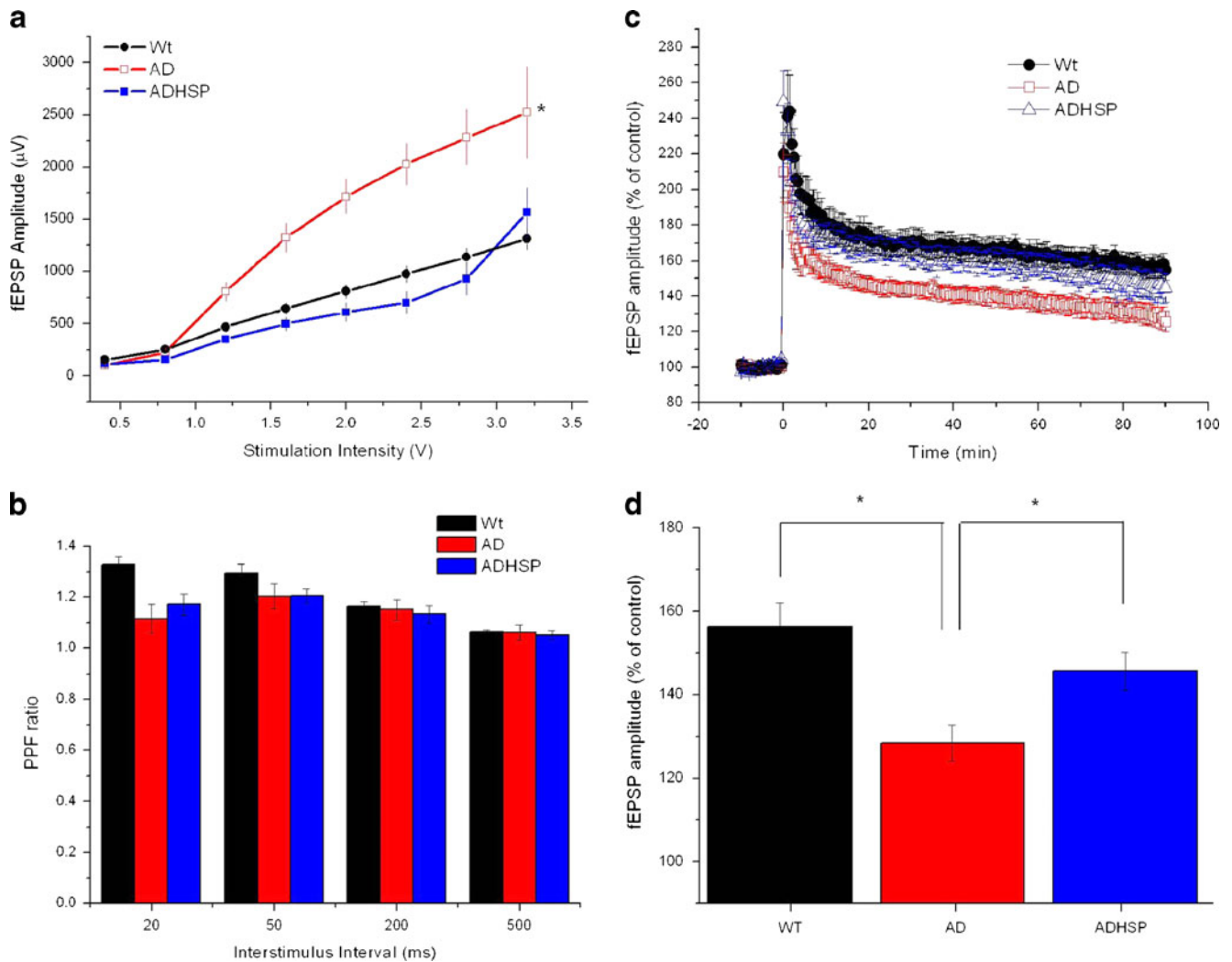
Fig. 3 Electrophysiological recordings on hippocampal slices from 7 months old mice. **a** Neuronal excitability of transgenic mice at different stimulation intensities. Data was analyzed by two-way ANOVA followed by Tukey's test. *Asterisk* denotes $p<0.05$. **b** Assessment of synaptic function in wild type (Wt, $n=8$), APPswe/PS1dE9 (AD, $n=6$), and APPswe/PS1dE9/Hsp27 (ADHSP, $n=7$) mice using PPF. There was no significant difference in PPF values of different genotypes. **c** TBS induced LTP in transgenic (AD and ADHSP) and wild type mice. **d** *Bar graph* shows the fEPSP amplitude means of the last 5 min of LTP. *Asterisk* denotes $p\le0.05$ analyzed by ANOVA and post hoc Bonferroni test

of neurons was studied at stimulation intensity of 0.4, 0.8, 1.2, 1.6, 2.0, 2.4, 2.8, and 3.2 V. Slices prepared from brains of AD model (APPswe/PS1dE9) mice showed an elevated fEPSP increase at the same stimulus intensity compared to control, indicating an increased excitability of neurons ($p\le0.05$, two-way ANOVA; Fig. 3a). This increased synaptic excitability was normalized in APPswe/PS1dE9/Hsp27 mice (Fig. 3a). However, paired-pulse facilitation did not differ significantly among the groups, indicating that presynaptic function was unaffected by the genotype (Fig. 3b).

LTP is a cellular correlate of learning and memory. We found that LTP was impaired in the APPswe/PS1dE9 group (125 ± 6 % vs. 154 ± 6 % in the wild type, $p\le0.05$), but this was partially rescued in the APPswe/PS1dE9/Hsp27 genotype mice (144 ± 8 %; Fig. 3c, d).

Amyloid staining

Amyloid plaque formation was studied by immunostaining of frozen brain sections of 7-month-old transgenic and wild type mice using anti-Aβ [1–42] antibody. Numerous amyloid deposits were observed in the hippocampus and cortex of APPswe/PS1dE9 transgenic animals (0.99/field of view and 1.08/field of view, respectively), in contrast to wild type animals (0.02/field of view in the hippocampus and 0.06/field of view in the cortex; Fig. 4a, b). Amyloid plaques were detected in APPswe/PS1dE9/Hsp27 brains as well (0.69/field of view in the hippocampus and 0.78/field of view in the cortex; Fig. 4a, b); however, the number of plaques was significantly less in both regions than in APPswe/PS1dE9 group ($p<0.05$; Fig. 4c), indicating that Hsp27 might prevent

amyloid aggregation and plaque formation, or it can facilitate amyloid clearance and degradation in the brain.
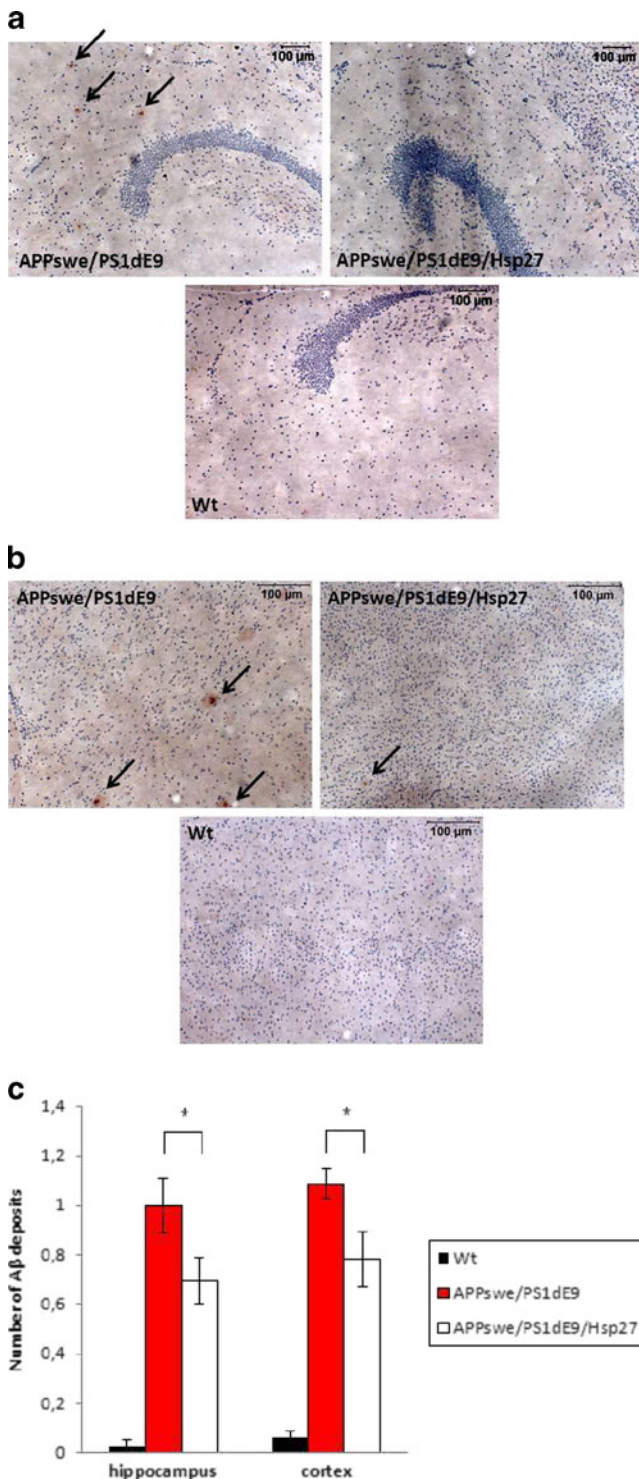

Fig. 4 Immunostaining of hippocampal (**a**) and cortical (**b**) amyloid plaques in 7 months old APPswe/PS1dE9, APPswe/PS1dE9/Hsp27 transgenic, and wild type (Wt) mice. *Arrows* indicate the presence of amyloid deposits. **c** Number of Aβ deposits/field of view in wild type (Wt, $n=6$), APPswe/PS1dE9 ($n=6$), and APPswe/PS1dE9/Hsp27 mice ($n=6$; mean ± SEM is shown; *$p<0.05$)

Neuronal apoptosis

We used anti-active caspase-3 antibody and Fluoro-Jade C stainings to monitor apoptosis and neurodegeneration in the brain of 7-month-old transgenic mice. Activation of effector caspase-3 molecules triggers the activation of caspase cascade, which eventually leads to apoptosis of the cells (Boatright and Salvesen 2003). Fluoro-Jade C is an anionic fluorochrome, which sensitively and specifically binds to degenerating neurons (Schmued et al. 2005). We detected significantly increased number of apoptotic cells (Fig. 5a) and degenerated neurons (Fig. 5b) in the hippocampal as well as cortical regions of APPswe/PS1dE9 and APPswe/PS1dE9/Hsp27 transgenic brains compared to wild type animals ($p<0.001$); however, there was no statistical difference between AD model mice and AD model mice expressing Hsp27.

Gene expression analysis of Hsp27 transgenic mice

Results obtained above indicated that Hsp27, as a molecular chaperone, might have a role in inhibition of amyloid
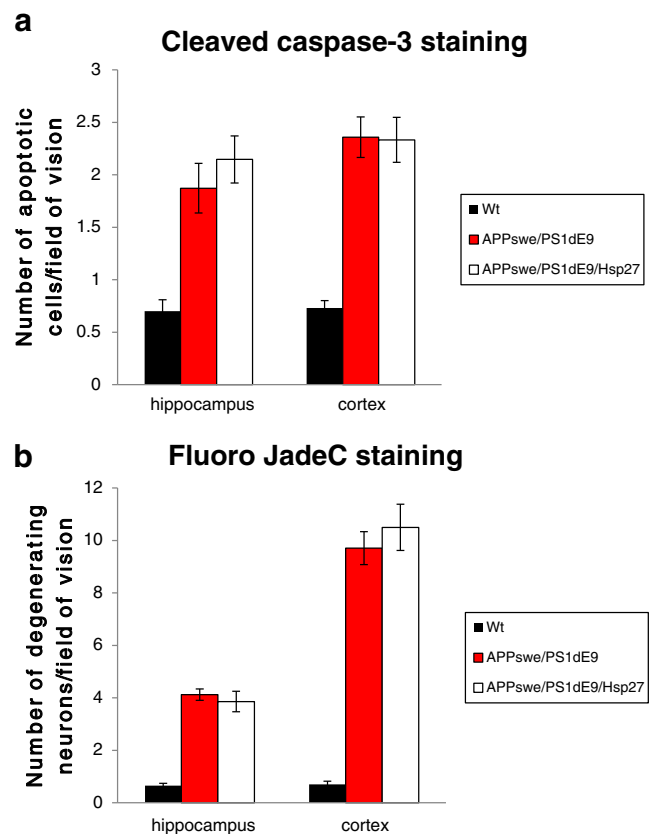

Fig. 5 Quantitative comparison of apoptotic cell (**a**) and degenerating neuron (**b**) numbers in the hippocampus and cortex of 7 months old wild type (Wt, $n=6$), APPswe/PS1dE9 ($n=6$), and APPswe/PS1dE9/Hsp27 ($n=6$) mice. Apoptotic cells were detected by anti-active caspase-3 antibody staining, while degenerating neurons were visualized using Fluoro-Jade C staining. Mean ± SEM is shown

accumulation/deposition or in enhanced amyloid clearing and degradation. In order to clarify its molecular role, we monitored the gene expression of several genes potentially involved in β-amyloid metabolism such as APP, ApoA1, ApoD, ApoE, LDLr, Lrp1, Lrp2, Hsp90, and neurodegeneration (NOS1 and NOS2) in the cortex of Hsp27 transgenic mice using Q-PCR. Primers used in this study are listed in Table 1. The expression level of ApoD and Lrp2 was slightly increased (128 % and 128 %, respectively), in the brain of Hsp27 transgenic mice compared to wild type controls (100 %), whereas there was no change in the mRNA level of APP, ApoE, LDLr, Lrp1, Hsp90, NOS1, and NOS3. Rather surprisingly, cortical expression of ApoA1 was reduced by half in Hsp27 transgenics versus wild type mice (Fig. 6a). Decreased ApoA1 expression in Hsp27 transgenic mice was further confirmed using western blotting. ApoA1 protein level was reduced in Hsp27 transgenic mice (61.1 %), but slightly elevated in AD model mice (126.7 %) compared to wild types (100 %). However, AD mice overexpressing human Hsp27 protein possessed similar ApoA1 protein level than wild type mice, indicating that Hsp27 influenced ApoA1 expression (Fig. 6b, c).

Discussion

In this study, we investigated the effects of small heat shock protein, Hsp27, on the development of AD-related phenotypes in transgenic mice. For this purpose, we used APPswe/PS1dE9 transgenic strain. These mice develop several AD-related phenotype including amyloid-beta deposits, abnormal spatial memory, axon degeneration, and synapse loss (The Jackson Laboratory (2013)) (http://jaxmice.jax.org/strain/004462.html). We overexpressed the human Hsp27 protein in AD model mice and monitored learning and memory, synaptic function, amyloid deposition, and neuronal apoptosis in the triple transgenic mice.

Decline of the short-term memory is among the primary symptoms in AD patients. We found that spatial learning was impaired in APPswe/PS1dE9 mice as the time required to find the escape hole in Barnes maze test, or the platform in Morris water maze test was significantly longer compared to wild type mice. However, the performance of APPswe/PS1dE9/Hsp27 group was similar to the wild type group in both tests, which suggests that overexpression of Hsp27 protein ameliorates learning and memory deficits.

We have also found that synaptic excitability was increased in AD model mice, but this was normalized by Hsp27 overexpression. This is in accordance with earlier findings of others who demonstrated that seizure susceptibility is increased in AD model mice (Westmark et al. 2008; Vogt et al. 2009), and heat shock proteins can moderate chemically induced seizures (Akbar et al. 2003; Ekimova et al. 2010). LTP, a cellular correlate of learning and memory (Bliss and Colingridge 1993), was also investigated on hippocampal slices. Previously, it was demonstrated that soluble oligomers of Aβ are able to inhibit LTP and cause learning and memory deficit (Haas and Selkoe 2007; Bozso et al. 2010). Our results have shown that LTP was impaired in APPswe/PS1dE9 mice indeed, but it was normalized upon Hsp27 overexpression. There is substantial evidence from transgenic mouse models that intracellular Aβ initiates cellular dysfunction, synaptic, electrophysiological, and behavioral changes before it accumulates in extracellular plaques (Moechars et al. 1999; Kumar-Singh et al. 2000; Mucke et al. 2000). The toxic Aβ molecules (either soluble oligomers or fibrillar forms) might initiate a cascade, which finally leads to neuronal dysfunction. Therefore, inhibition of Aβ oligomerization and deposition or enhanced clearance of Aβ might play a crucial role in the prevention and therapy of AD. We have found a significantly lower level of amyloid deposition in the brain of AD/Hsp27 animals compared to the AD group, indicating that Hsp27 is somehow involved in these processes. In AD, heat shock protein expression is associated with Aβ deposition and neurofibrillary tangles, and recent findings suggest that Hsps prevent the accumulation of Aβ (Abdul et al. 2006; Evans et al. 2006). Wilhelmus et al. (2006) demonstrated that Hsp20, Hsp27, and αB-crystallin bind strongly to Aβ and inhibit its aggregation. Furthermore, Hsp20, Hsp27, and αB-crystallin inhibited cerebrovascular Aβ toxicity, probably by reducing the accumulation of Aβ at the cell surface.

Aggregated forms of Aβ might lead to neurodegeneration through different pathways. Several studies have shown that chronic inflammatory response to deposited amyloid resulted in neurodegeneration (Akiyama et al. 2000; Wyss-Coray and Mucke 2002). Although heat shock proteins have protective effects in neurodegenerative disease models, the molecular basis of this protection is not fully understood. It is likely that heat shock proteins have effect at several levels, and their neuroprotective function might not be linked exclusively to their effect on protein aggregation (Muchowski and Wacker 2005). For example, Hsps are known to reduce oxidative stress and mediate apoptotic pathway. They can also facilitate proteasomal degradation, which might help in Aβ clearance. However, the exact molecular mechanisms of Aβ-induced neurotoxicity are not fully known. These mechanisms are very diverse, and probably include the increased production of reactive oxygen species (ROS), altered calcium homeostasis, and enzyme activities. Several lines of evidence are available suggesting that Aβ can interact with artificial and biological membranes altering their fluidity. Altered membrane fluidity can influence the function of other membrane components. Certain studies suggest that the insertion of Aβ into the plasma membrane triggers different events catalyzed by perturbation of the conformation of membrane proteins, which finally leads to neurotoxicity (Kanfer et al. 1999). This

Fig. 6 Gene expression profiles of different genes involved in amyloid metabolism in Hsp27 transgenic mice using Q-PCR analysis (**a**). Data was normalized to the endogenous β-actin, then expressed as a percent of wild type expression (100 %). **b** Representative western blot of ApoA1 expression in Hsp27 transgenic (Hsp27), wild type (Wt), AD model (APPswe/PS1dE9), and AD/Hsp27 (APPswe/PS1dE9/Hsp27) brains. **c** Statistical analysis of western blot experiment. Hsp27 transgenic (*n*=5), wild type (Wt, *n*=6), AD model (*n*=5), and AD/Hsp triple transgenic mice (*n*=6) were compared
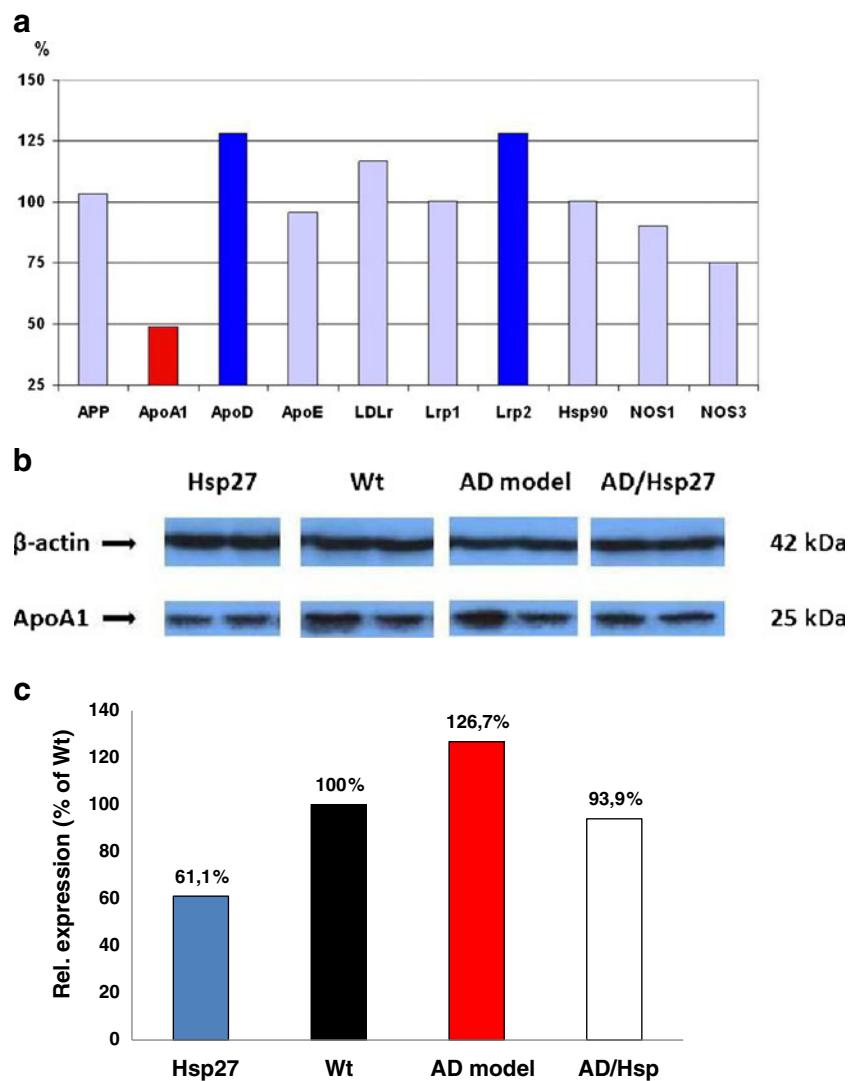
hypothesis suggests that the neurotoxic cascade of Aβ is initiated in the cell membrane. It is also important, that α-, β-, and γ-secretases are associated with cellular membranes; thereby, their function, such as APP processing, strongly depends on membrane fluidity. Peters et al. (2009) showed that oligomeric Aβ can reduce membrane fluidity, which in turn stimulates the amyloidogenic processing of APP. Several studies suggest that a subpopulation of Hsps is present either on the surface or within the cellular membranes, and they have been shown to modulate major attributes of the membrane lipid phase such as fluidity and permeability. By stabilizing the membrane, Hsps can restore membrane functionality during stress conditions (Horváth et al. 2008). We can suppose that Hsp27 also can interact with and stabilize cellular membranes; thereby, it can diminish the level of Aβ-induced neurotoxic cascade or, moreover, the production of Aβ. The generation of ROS is also a crucial factor in the molecular mechanisms of Aβ-induced neurotoxicity. Lipid peroxidation,

and protein and DNA oxidation are remarkable in the brain of AD patients, and Aβ might have a central role in the induction of these processes (reviewed in Butterfield et al. 2001). Hsp27 has a protective effect in oxidative stress; thereby, Hsp27 might eliminate the neurotoxicity of Aβ at least in part due to this property.

To know more about the role of Hsp27 in amyloid metabolism—whether it inhibits APP production or enhances amyloid clearance/degradation—we performed gene expression analysis. No decrease in APP production was detected; however, a subtle elevation of ApoD and LRP1 protein levels in Hsp27 transgenic brains was observed. Although ApoD and LRP1 proteins have important roles in neuroprotection and Aβ clearance, respectively (Terrise at al. 1998; Kalman et al. 2000; Thomas et al. 2001; Muffat et al. 2008; Kang et al. 2000), we do not consider that the mild changes obtained in their expression would be sufficiently enough to lead to efficient reduction of amyloid plaque

numbers. Now it is widely accepted that ApoD is elevated in many neuropathological conditions, including Alzheimer's disease, Parkinson's disease, stroke, schizophrenia, and bipolar disorder. It was also demonstrated that in *Drosophila*, overexpressed ApoD had a protective effect against oxidative stress and heat shock (Muffat et al. 2008). In vitro LDL receptor-related protein 1 (LRP1) mediates the clearance of both Aβ 40 and Aβ 42 through a bona fide receptor-mediated uptake (Kang et al. 2000); therefore, LRP and its ligand ApoE have been proposed to be a clearance pathway for Aβ. At the same time, the role of ApoA1 in amyloid metabolism and AD pathology is controversial. Although it has been shown that ApoA1 inhibits Aβ aggregation in vitro (Koldamova et al. 2001), in vivo studies resulted different results. Crossing of ApoA1 null mice with AD model mice resulted no change in amyloid deposition in the brain (Fagan et al. 2004). Similarly, when ApoA1 overexpressing mice were crossed with AD model mice, no alteration in amyloid metabolism was observed (Lewis et al. 2010). Our result presented here shows that expression of ApoA1 was downregulated in Hsp27 transgenic mice, indicating that Hsp27 might have a role in the regulation (directly or indirectly) of ApoA1 expression.

Taken together, further investigations are necessary to reveal the exact molecular pathways involved in neuroprotective function of Hsp27.

Conflicts of interest   The authors declare no competing financial interests.

References

Abdul HM, Calabrese V, Calvani M, Butterfield DA (2006) Acetyl-L-carnitine-induced up-regulation of heat shock proteins protects cortical neurons against amyloid-beta peptide 1-42-mediated oxidative stress and neurotoxicity: implications for Alzheimer's disease. J Neurosci Res 84:398–408

Akbar MT, Lundberg AM, Liu K, Vidyadaran S, Wells KE, Dolatshad H, Wynn S, Wells DJ, Latchman DS, de Belleroche J (2003) The neuroprotective effects of heat shock protein 27 overexpression in transgenic animals against kainate-induced seizures and hippocampal cell death. J Biol Chem 278:19956–19965

Akiyama H, Barger S, Barnum S, Bradt B, Bauer J, Cole GM, Cooper NR, Eikelenboom P et al (2000) Inflammation and Alzheimer's disease. Neurobiol Aging 21:383–421

Arrigo AP, Paul C, Ducasse C, Manero F, Kretz-Remy C, Virot S, Javouhey E, Mounier N, Diaz-Latoud C (2002) Small stress proteins: novel negative modulators of apoptosis induced independently of reactive oxygen species. Prog Mol Subcell Biol 28:185–204

Becker J, Craig EA (1994) Heat-shock proteins as molecular chaperones. Eur J Biochem 219:11–23

Bliss TVP, Collingridge GL (1993) A synaptic model of memory: long-term potentiation in the hippocampus. Nature 361:31–39

Boatright KM, Salvesen GS (2003) Mechanisms of caspase activation. Curr Opin Cell Biol 15:725–731

Bozso Z, Penke B, Simon D, Laczkó I, Juhász G, Szegedi V, Kasza A, Soós K, Hetényi A, Wéber E, Tóháti H, Csete M, Zarándi M, Fülöp L (2010) Controlled in situ preparation of A beta(1–42) oligomers from the isopeptide "iso-A beta(1–42)" physicochemical and biological characterization. Peptides 31:248–256

Butterfield DA, Drake J, Pocernich C, Castegna A (2001) Evidence of oxidative damage in Alzheimer's disease brain: central role for amyloid beta-peptide. Trends Mol Med 7:548–554

Ekimova IV, Nitsinskaya LE, Romanova IV, Pastukhov YF, Margulis BA, Guzhova IV (2010) Exogenous protein Hsp70/Hsc70 can penetrate into brain structures and attenuate the severity of chemically-induced seizures. J Neurochem 115:1035–1044

Evans CG, Wisen S, Gestwicki JE (2006) Heat shock proteins 70 and 90 inhibit early stages of amyloid beta-(1–42) aggregation in vitro. J Biol Chem 281:33182–33191

Evans DA, Funkenstein HH, Albert MS, Scherr PA, Cook NR, Chown MJ, Hebert LE, Hennekens CH, Taylor JO (1989) Prevalence of Alzheimer's disease in a community population of older persons. Higher than previously reported. JAMA 262:2551–2556

Fagan AM, Christopher E, Taylor JW, Parsadanian M, Spinner M, Watson M, Fryer JD, Wahrle S, Bales KR, Paul SM, Holtzman DM (2004) ApoAI deficiency results in marked reductions in plasma cholesterol but no alterations in amyloid-beta pathology in a mouse model of Alzheimer's disease-like cerebral amyloidosis. Am J Pathol 165:1413–1422

Haass C, Selkoe DJ (2007) Soluble protein oligomers in neurodegeneration: lessons from the Alzheimer's amyloid beta-peptide. Nat Rev Mol Cell Biol 8:101–112

Hamilton A, Holscher C (2012) The effect of ageing on neurogenesis and oxidative stress in the APP(swe)/PS1(deltaE9) mouse model of Alzheimer's disease. Brain Res 1449:83–93

Haslbeck M, Buchner J (2002) Chaperone function of sHSPs. Prog Mol Subcell Biol 28:37–59

Horváth I, Multhoff G, Sonnleitner A, Vígh L (2008) Membrane-associated stress proteins: more than simply chaperones. Biochim Biophys Acta 1778:1653–1664

Hoshino T, Murao N, Namba T, Takehara M, Adachi H, Katsuno M, Sobue G, Matsushima T, Suzuki T, Mizushima T (2011) Suppression of Alzheimer's disease-related phenotypes by expression of heat shock protein 70 in mice. J Neurosci 31:5225–5234

Jakob U, Gaestel M, Engel K, Buchner J (1993) Small heat shock proteins are molecular chaperones. J Biol Chem 268:1517–1520

Jankowsky JL, Fadale DJ, Anderson J, Xu GM, Gonzales V, Jenkins NA, Copeland NG, Lee MK, Younkin LH, Wagner SL, Younkin SG, Borchelt DR (2004) Mutant presenilins specifically elevate the levels of the 42 residue beta-amyloid peptide in vivo: evidence for augmentation of 42-specific gamma secretase. Hum Mol Genet 13:159–170

Kalman J, McConathy W, Araoz C, Kasa P, Lacko AG (2000) Apolipoprotein D in the aging brain and in Alzheimer's dementia. Neurol Res 22:330–336

Kalmar B, Greensmith L (2009) Induction of heat shock proteins for protection against oxidative stress. Adv Drug Deliv 61:310–318

Kanfer JN, Sorrentino G, Sitar DS (1999) Amyloid beta peptide membrane perturbation is the basis for its biological effects. Neurochem Res 24:1621–1630

Kang DE, Pietrzik CU, Baum L, Chevallier N, Merriam DE, Kounnas MZ, Wagner SL, Troncoso JC, Kawas CH, Katzman R, Koo EH (2000) Modulation of amyloid beta-protein clearance and Alzheimer's disease susceptibility by the LDL receptor-related protein pathway. J Clin Invest 106:1159–1166

Katsuno M, Sang C, Adachi H, Minamiyama M, Waza M, Tanaka F, Doyu M, Sobue G (2005) Pharmacological induction of heat-shock proteins alleviates polyglutamine-mediated motor neuron disease. Proc Natl Acad Sci U S A 102:16801–16806

Kennard JA, Woodruff-Pak DS (2011) Age sensitivity of behavioral tests and brain substrates of normal aging in mice. Front Aging Neurosci 3:9

Koldamova RP, Lefterov IM, Lefterova MI, Lazo JS (2001) Apolipoprotein A-I directly interacts with amyloid precursor protein and inhibits A beta aggregation and toxicity. Biochemistry 40:3553–3560

Kumar-Singh S, Dewachter I, Moechars D, Lübke U, De Jonghe C, Ceuterick C, Checler F, Naidu A, Cordell B, Cras P, Van Broeckhoven C, Van Leuven FS (2000) Behavioral disturbances without amyloid deposits in mice overexpressing human amyloid precursor protein with Flemish (A692G) or Dutch (E693Q) mutation. Neurobiol Dis 7:9–22

Lewis TL, Cao D, Lu H, Mans RA, Su YR, Jungbauer L, Linton MF, Fazio S, Ladu MJ, Li L (2010) Overexpression of human apolipoprotein A-I preserves cognitive function and attenuates neuroinflammation and cerebral amyloid angiopathy in a mouse model of Alzheimer's disease. J Biol Chem 285:36958–36968

Lo Bianco C, Shorter J, Régulier E, Lashuel H, Iwatsubo T, Lindquist S, Aebischer P (2008) Hsp104 antagonizes alpha-synuclein aggregation and reduces dopaminergic degeneration in a rat model of Parkinson disease. J Clin Invest 118:3087–3097

Magrané J, Smith RC, Walsh K, Querfurth HW (2004) Heat shock protein 70 participates in the neuroprotective response to intracellularly expressed β-amyloid in neurons. J Neurosci 24:1700–1706

Mattson MP (2004) Pathways towards and away from Alzheimer's disease. Nature 430:631–639

McKhann G, Drachman D, Folstein M, Katzman R, Price D, Stadlan EM (1984) Clinical diagnosis of Alzheimer's disease: report of the NINCDS-ADRDA Work Group under the auspices of Department of Health and Human Services Task Force on Alzheimer's Disease. Neurology 34:939–944

Moechars D, Dewachter I, Lorent K, Reversé D, Baekelandt V, Naidu A, Tesseur I, Spittaels K, Haute CV, Checler F, Godaux E, Cordell B, Van Leuven F (1999) Early phenotypic changes in transgenic mice that overexpress different mutants of amyloid precursor protein in brain. J Biol Chem 274:6483–6492

Monji A, Utsumi H, Ueda T, Imoto T, Yoshida I, Hashioka S, Tashiro K, Tashiro N (2001) The relationship between the aggregational state of the amyloid-beta peptides and free radical generation by the peptides. J Neurochem 77:1425–1432

Morimoto RI, Sarge KD, Abravaya K (1992) Transcriptional regulation of heat shock genes. A paradigm for inducible genomic responses. J Biol Chem 267:21987–21990

Muchowski PJ, Wacker JL (2005) Modulation of neurodegeneration by molecular chaperones. Nat Rev Neurosci 6:11–22

Mucke L, Masliah E, Yu GQ, Mallory M, Rockenstein EM, Tatsuno G, Hu K, Kholodenko D, Johnson-Wood K, McConlogue L (2000) High-level neuronal expression of Aβ 1–42 in wild-type human amyloid protein precursor transgenic mice: synaptotoxicity without plaque formation. J Neurosci 20:4050–4058

Muffat J, Walker DW, Benzer S (2008) Human ApoD, an apolipoprotein up-regulated in neurodegenerative diseases, extends lifespan and increases stress resistance in Drosophila. Proc Natl Acad Sci U S A 105:7088–7093

Perez N, Sugar J, Charya S, Johnson G, Merril C, Bierer L, Perl D, Haroutunian V, Wallace W (1991) Increased synthesis and accumulation of heat shock 70 proteins in Alzheimer's disease. Brain Res Mol Brain Res 11:249–254

Peters I, Igbavboa U, Schütt T, Haidari S, Hartig U, Böttner S, Copanaki E, Deller T, Kögel D, Wood WG, Müller WE, Eckert GP (2009) The interaction of beta-amyloid protein with cellular membranes stimulates its own production. Biochim Biophys Acta 1788:964–972

Preville X, Salvemini F, Giraud S, Chaufour S, Paul C, Stepien G, Ursini MV, Arrigo AP (1999) Mammalian small stress proteins protect against oxidative stress through their ability to increase glucose-6-phosphate dehydrogenase activity and by maintaining optimal cellular detoxifying machinery. Exp Cell Res 247:61–78

Reiserer RS, Harrison FE, Syverud DC, McDonald MP (2007) Impaired spatial learning in the APP + PSEN1DeltaE9 bigenic mouse model of Alzheimer's disease. Genes Brain Behav 6:54–65

Schmued LC, Stowers CC, Scallet AC, Xu L (2005) Fluoro-Jade C results in ultra high resolution and contrast labeling of degenerating neurons. Brain Res 1035:24–31

Serrano-Pozo A, Frosch MP, Masliah E, Hyman BT (2011) Neuropathological alterations in Alzheimer disease. Cold Spring Harb Perspect Med 1(1):a006189

Sunyer B, Patil S, Höger H, Lubec G (2007) Barnes maze, a useful task to assess spatial reference memory in the mice. Protocol Exchange. doi:10.1038/nprot.2007.390

Terrisse L, Poirier J, Bertrand P, Merched A, Visvikis S, Siest G, Milne R, Rassart E (1998) Increased levels of apolipoprotein D in cerebrospinal fluid and hippocampus of Alzheimer's patients. J Neurochem 71:1643–1650

The Jackson Laboratory (2013) http://jaxmice.jax.org/strain/004462.html

Thomas EA, Dean B, Pavey G, Sutcliffe JG (2001) Increased CNS levels of apolipoprotein D in schizophrenic and bipolar subjects: implications for the pathophysiology of psychiatric disorders. Proc Natl Acad Sci U S A 98:4066–4071

Toth ME, Gonda S, Vigh L, Santha M (2010) Neuroprotective effect of small heat shock protein, Hsp27, after acute and chronic alcohol administration. Cell Stress Chaperones 15:807–817

Vogt DL, Thomas D, Galvan V, Bredesen DE, Lamb BT, Pimplikar SW (2009) Abnormal neuronal networks and seizure susceptibility in mice overexpressing the APP intracellular domain. Neurobiol Aging 32:1725–1729

Wang K, Spector A (1996) α-Crystallin stabilizes actin filaments and prevents cytochalasin-induced depolymerization in a phosphorilation-dependent manner. Eur J Biochem 242:56–66

Westmark CJ, Westmark PR, Beard AM, Hildebrandt SM, Malter JS (2008) Seizure susceptibility and mortality in mice that over-express amyloid precursor protein. Int J Clin Exp Pathol 1:157–168

Wilhelmus MM, Boelens WC, Otte-Höller I, Kamps B, de Waal RM, Verbeek MM (2006) Small heat shock proteins inhibit amyloid-beta protein aggregation and cerebrovascular amyloid-beta protein toxicity. Brain Res 1089:67–78

Wyss-Coray T, Mucke L (2002) Inflammation in neurodegenerative disease—a double-edged sword. Neuron 35:419–432